Micromagnetic Dynamics in Field-Free Magnetization Switching Assisted by Interlayer Dzyaloshinskii–Moriya Interaction

Cuixiu Zheng[1], Wenqing He[2], Mo Zhu[1], Caihua Wan[2], Xiufeng Han[2,*], and Yaowen Liu [1,3,*]

[1]*School of Physics Science and Engineering, Tongji University, Shanghai 200092, China.*

[2]*Beijing National Laboratory for Condensed Matter Physics, Institute of Physics, University of Chinese Academy of Sciences, Chinese Academy of Sciences, Beijing 100190, China*

[3]*Shanghai Key Laboratory for Special Artificial Microstructure Materials and Technology, Tongji University, Shanghai 200092, China.*

Supplementary Materials

Experimental demonstrations of the field-free SOT switching assisted by iDMI are conducted in Pt/Co/Pt/Co/Pt and Pt/Co/Pt/Ir(1.3)/Pt/Co/Pt stacks [1]. These stacks are grown under a small in-plane field (H_{in}), exhibiting ferromagnetic or antiferromagnetic coupling between two Co layers. Figure 1 shows a typical sample with a structure of Pt(2)/[Co(0.4)/Pt(0.7)/Co(0.4)]/Pt(2) (unit in nm). The sample exhibits an out-of-plane easy axis due to the high interfacial PMA of Pt/Co and Co/Pt. To determine the direction of the iDMI vector (***D***), the loop-shift method [2] is employed. The anomalous Hall resistance signal (R_{AHE}) is measured as a function of out-of-plane field (H_z) at a fixed H_{in} (10 Oe) while rotating the sample in-plane. The rotation angle is described by an azimuth angle φ. The effective fields ($H_{DM,T}$ and $H_{DM,B}$) acting on the top and bottom Co layers depend on the orientation of ***D*** with respect to H_{in}. When ***D*** is perpendicular to H_{in}, the effective field ($H_{DM,T}$ and $H_{DM,B}$) are both maximized, causing substantial shift in the R_{AHE} vs H_z curves away from the H_z=0 axis [Figure 1(a)]. Conversely, while ***D*** is aligned collinearly with H_{in}, the $H_{DM,T}$ and $H_{DM,B}$ are both minimized, eliminating the shift in the R_{AHE} vs H_z curves. Based on this behavior, the switching fields H_{sw}^{UD} and H_{sw}^{DU}, representing the transition from spin-up to spin-down state and vice versa, can be extracted from each R_{AHE} vs H_z curve. The azimuthal angle dependence of $|H_{sw}|$ is summarized in Figure 1(b). It reveals that the maximum value of $|H_{sw}^{DU}|$ and H_{sw}^{UD} appears at φ=90° and 270° (anti-symmetric axis) and the minimum values are found at

* Authors to whom correspondence should be addressed. Email: xfhan@iphy.ac.cn; yaowen@tongji.edu.cn

φ=0° and 360° direction (symmetric axis). This observation indicates that the ***D*** vector of the stack deviates from the current channel of the crossbar by 90°.

To further validate the physics of iDMI-assisted SOT switching, both the parallel and orthogonal configurations between the applied current I and the ***D*** vector are considered. When the current is applied parallel to the ***D*** vector, we observe the deterministic field-free SOT switching curves characterized by odd symmetry, as depicted in Figure 1(c). Conversely, when the current is oriented perpendicular to the D vector, such switching is notably absent, as shown in Figure 1(d). This dichotomy underscores the critical role of the current's alignment with the ***D*** vector in facilitating or inhibiting the SOT switching process, thereby highlighting the nuanced interplay between spin-orbit torque and iDMI in achieving effective magnetization control.

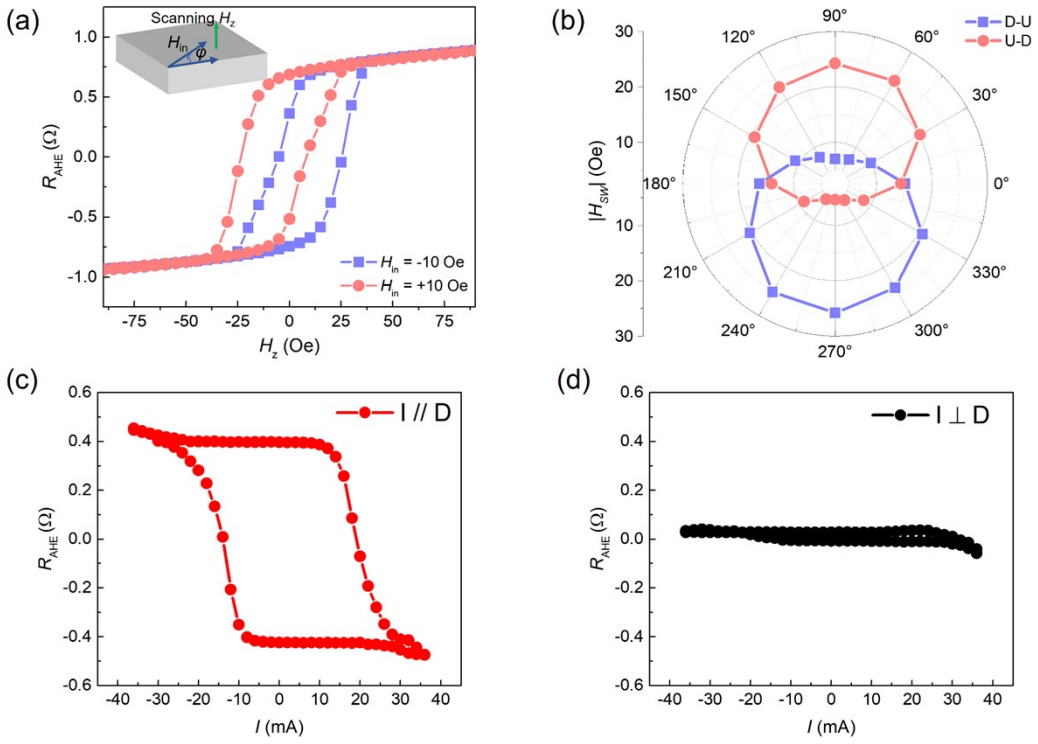

Supp. Fig. S1: **(a)** Typical out-of-plane hysteresis loop of the Pt(2)Co(0.4)Pt(0.7)Co(0.4)Pt(2 nm) sample at azimuth angle φ = 270° and φ = 90°. **(b)** Polar diagrams illustrating the switching field H_{sw} as a function of the φ angle of the in-plane field for the samples. **(c, d)** Field-free SOT switching for the samples with current parallel to the DMI vector (**I//D)** and current perpendicular to the DMI vector (**I⊥D)**, respectively. For **I//D**, switching loops with odd symmetry were observed, while switching was absent at **I⊥D.**

To address this, we conducted additional simulations, extending the pulse widths range from t_{pulse}=0.1 ns to t_{pulse}=1.2 ns (short pulses), which is now detailed in Supp. Fig. S2. These simulations reveal that for very short pulses (t_{pulse}= 0.1~0.8 ns), the in-

plane polarized current does not persist long enough to fully overcome the perpendicular anisotropy to drive magnetization to the m_z=0 plane. As a result, the magnetization remains in the m_z>0 plane after the current pulse is removed, where the perpendicular anisotropy ultimately drives the magnetization to the +z direction.

Conversely, for longer pulse durations (t_{pulse}>0.8 ns), the magnetization is sufficiently compressed within the m_z=0 plane, allowing the iDMI to dominant and determine the final magnetic orientation. Thus, applying longer pulses improves the likelihood of achieving deterministic iDMI-based magnetization switching, which we believe is promising for practical applications.

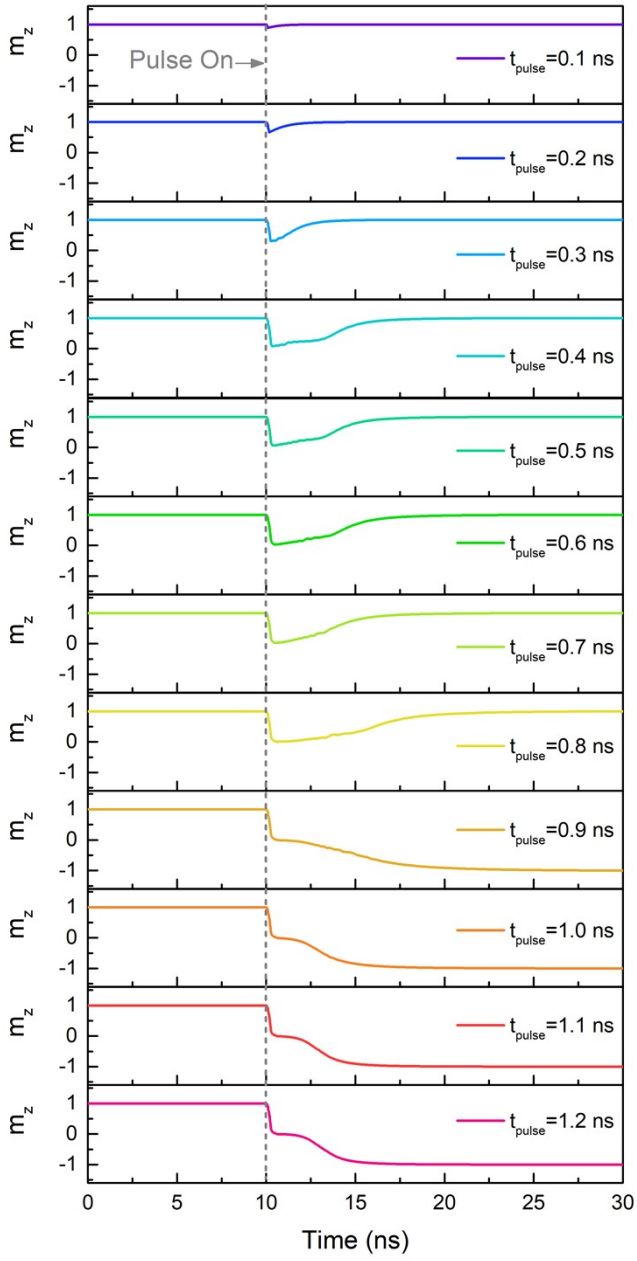

Supp. Fig. S2: Evolution of m_z induced for different current pulse widths with a damping factor

α=0.05 in FM sample.

To study the impact of more factors, we have performed a series of micromagnetic simulations in which the temperature variations, external magnetic fields and material properties have been taken into account.

Temperature variations: We explored the effect of temperature variations from 100K to 300K, as shown in Supp. Fig. S3 (a). The inset highlights the first 5 ns of magnetization evolution, showing the thermal noise amplitude increases with temperature, causing longer switching time. This demonstrates that higher temperatures could impede rapid switching, slightly affecting the device performance under realistic operational conditions.

External magnetic fields: As shown in Supp. Fig. S3(b), we examined the response of magnetization switching under different magnetic fields in the $\pm z$ direction. Applying current pulses under these fields cause the magnetization to deviate from the in-plane orientation, with the final magnetization direction aligning entirely with the extneral field direction. This result indicates that the external magnetic field directly drives the switching behavior, effectively driving the magnetization instead of achieving field-free switching. As such, magnetization switching under an applied magnetic field deviates from our study's focus on field-free switching, but we have included this analysis in the supplementary materials to clarify the impact of external fields and address the reviewer's query comprehensively.

Furthermore, to represent the material imperfections, we introduced an asymmetry factor, Λ, which accounts for device geometry and the physical properties of FM layers and interfaces. As seen in Supp. Fig. S3 (c), deterministic magnetization switching occurs when $\Lambda \geq 2$ (matching the original simulation, Λ=2, as noted in the revised manuscript on Page 4). Additionally, increasing Λ could speed up deterministic switching.

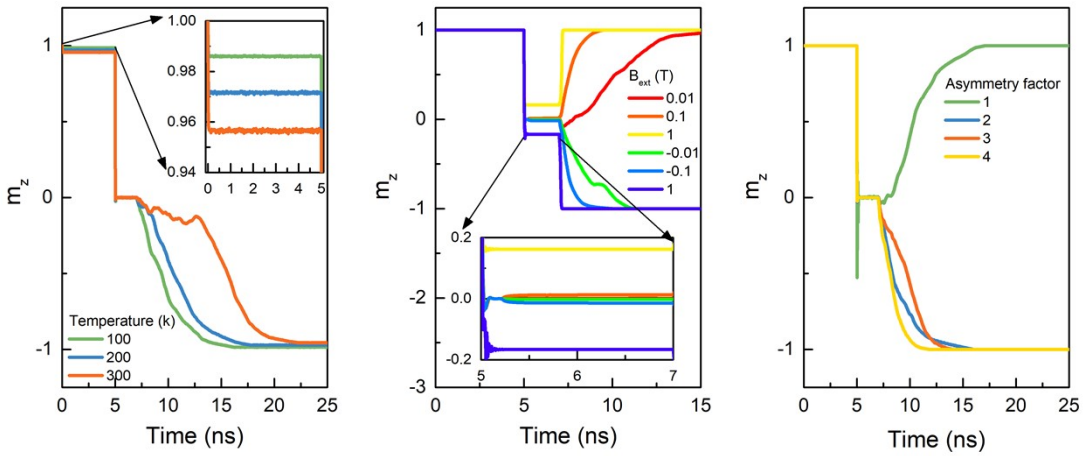

Supp. Fig. S3: Dependence of time evolution in the FM coupling sample on asymmetry factor Λ (a), temperature (b) and external magnetic fields(c).

1. W. He, C. Wan, C. Zheng, Y. Wang, X. Wang, T. Ma, Y. Wang, C. Guo, X. Luo, M. E. Stebliy, G. Yu, Y. Liu, A. V. Ognev, A. S. Samardak and X. Han, *Nano. Lett.*, 2022, **22**, 6857-6865.
2. D.-S. Han, K. Lee, J.-P. Hanke, Y. Mokrousov, K.-W. Kim, W. Yoo, Y. L. W. van Hees, T.-W. Kim, R. Lavrijsen, C.-Y. You, H. J. M. Swagten, M.-H. Jung and M. Kläui, *Nat. Mater.*, 2019, **18**, 703-708.